Marine Geology 406 (2018) 119–131

Contents lists available at ScienceDirect

Marine Geology

journal homepage: www.elsevier.com/locate/margo

Particle fluxes induced by benthic storms during the 2012 dense shelf water cascading and open sea convection period in the northwestern Mediterranean basin

Albert Palanques*, Pere Puig

Institut de Ciències del Mar (CSIC), Passeig Maritim de la Barceloneta, 37-49, Barcelona 08003, Spain

ARTICLE INFO

Editor: Michele Rebesco

Keywords:
Benthic storms
Open sea convection
Dense shelf water cascading
Deep sea
Sediment transport
Seafloor resuspension

ABSTRACT

The effects of deep dense shelf water cascading and open sea convection on the sediment dynamics of the northwestern Mediterranean basin were studied by near-bottom moored instruments recording trapped particle fluxes, suspended particle fluxes, water properties and hydrodynamics from November 2011 to July 2012. During this period, near-bottom currents induced by winter dense water formation generated benthic storms that caused resuspension at 2450 m water depth, increasing by more than one order of magnitude the ambient suspended sediment concentrations, the trapped particle fluxes and the suspended sediment fluxes. During the preconditioning phase of the open sea convection, from December 2011 to mid-February 2012, currents (1–10 cm s^{-1}), suspended sediment concentrations (< 0.1 mg l^{-1}), Chl-a fluorescence values (< 0.063 µg l^{-1}), trapped total mass fluxes (10–50 mg m^{-2} d^{-1}) and trapped organic carbon fluxes (1–4 mg m^{-2} d^{-1}) were low, and organic matter was mainly undegraded and of marine origin. Open sea convection was observed at the study site in mid-February, at the beginning of the violent mixing phase, increasing current velocities up to 26 cm s^{-1} and Chl-a fluorescence values up to 0.074 µg l^{-1}, supplying particles with fresh marine organic matter content. During the last fortnight of February, two major dense shelf water cascading pulses generated Chl-a fluorescence increases (up to 0.116 µg l^{-1}) and large suspended sediment concentration peaks (up to19 mg l^{-1}), suspended sediment fluxes (up to 6500 mg m^{-2} d^{-1}) and trapped total mass flux increases (up to 22,900 mg m^{-2} d^{-1}), which were associated with benthic storms resuspension. During this phase, trapped organic carbon flux increased almost two orders of magnitude (up to 260 mg m^{-2} d^{-1}), with pulses of both marine and terrestrial organic matter. The sinking and spreading phase occurred from early March to mid-June. The signal of deep dense shelf water cascading lasted past early April, and the spreading of the newly formed dense water maintained maximum currents of up to 25 cm s^{-1} and trapped particle fluxes of up to 2000 mg m^{-2} d^{-1} until mid-June. At the beginning of this phase, organic matter was terrestrial and several turbidity peaks occurred during current speed increases generated by benthic storms. At the end of this phase, the organic matter became less terrestrial, trapped organic carbon fluxes decreased from about 190 to 10 mg m^{-2} d^{-1} and turbidity peaks occurred with low current velocities indicating the arrival of storm tails at the mooring site. The large particle fluxes of fresh or relatively undegraded organic carbon induced by deep dense water formation during winter 2012, contributed to the "fertilization" of the northwestern Mediterranean deep benthic ecosystems.

1. Introduction

In the northwestern Mediterranean, dense water formation is produced by surface cooling and evaporation in wintertime due to cold and dry northerly (Mistral) and northwesterly (Tramontane) winds, which cause strong densification and homogenization of the surface-water column (MEDOC group, 1970; Millot, 1990; Durrieu de Madron et al., 2005). This phenomenon occurs both in coastal waters on the Gulf of Lions, causing dense shelf water cascading (DSWC) and on the central part of the northwestern Mediterranean basin, causing open sea convection (OSC). The amount of dense waters formed in each region and their characteristics show a high interannual variability depending on the wind intensity and persistence, on the freshwater inputs preventing DSWC and also on the preconditioning of the water column (Estournel et al., 2003; L'Heveder et al., 2013).

It is well known that in the northwestern Mediterranean OSC occurs

* Corresponding author.
E-mail address: albertp@icm.csic.es (A. Palanques).

https://doi.org/10.1016/j.margeo.2018.09.010
Received 13 April 2018; Received in revised form 12 August 2018; Accepted 16 September 2018
Available online 21 September 2018

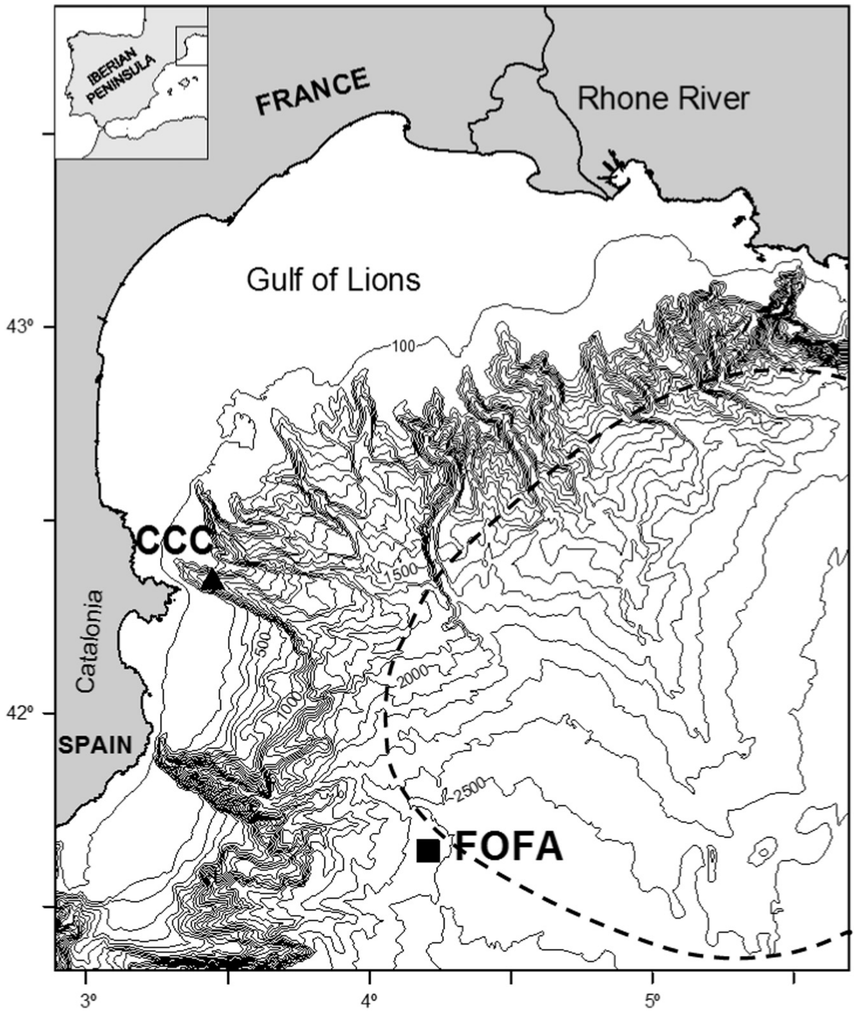

Fig. 1. General bathymetric map of the Gulf of Lions and the northern Catalan Sea, showing the location of the FOFA and the Cap de Creus Canyon (CCC) sites where moorings were deployed. The dashed line shows the area of deep Open-Sea Convection (Houpert et al., 2016).

in three stages or phases. First, there is a weakening of the vertical stratification known as the "preconditioning" phase (Stommel, 1972). It is followed by the homogenization of the water column in various chimneys distributed within the preconditioning area, during a period known as the "violent mixing phase" (Marshall and Schott, 1999). The third stage is the "sinking and spreading phase" (Killworth, 1976), during which dense water fills the deep basin below 1000 m (MEDOC group, 1970; Schott and Leaman, 1991). This spreading mainly results from the action of anticyclonic submesoscale coherent vortices (radius about 5 km and life time > 0.5 years) that can advect lenses of deep water several hundreds of kilometers away from the formation area (Testor and Gascard, 2003, 2006; Houpert et al., 2016).

Concurrent with the OSC process, the dense water is formed over the Gulf of Lions shelf and subsequently cascades downslope across the Gulf of Lions and northern Catalan margins, being mainly channelized through submarine canyons (Palanques et al., 2006; Canals et al., 2006; Puig et al., 2008; Ribó et al., 2011). Dense shelf water flows can reach $\sim 1\ \mathrm{m\,s^{-1}}$ and erode and reshape the seafloor, particularly within submarine canyon axes, increasing their suspended and bed load sediment transport as they progress from the shelf edge towards the slope and basin (Canals et al., 2006; Puig et al., 2008; Palanques et al., 2008, 2012; Ogston et al., 2008). Resuspended sediments by DSWC can be detached at the neutral buoyancy level, forming intermediate nepheloid layers, or evolve into a thick bottom nepheloid layer towards the basin (Puig et al., 2013). This suspended particulate matter transfer plays an important role in biogeochemical cycles by exporting phytoplankton and organic matter from shallow productive areas towards deep sea environments (Sanchez-Vidal et al., 2009; Pasqual et al., 2010; Palanques et al., 2011; Tesi et al., 2010), which can ultimately affect the life histories of deep-sea megafauna populations (Company et al., 2008).

Mixing of deep cascading and convection dense waters occurs at a subdecadal recurrence, when atmospheric forcing is intense enough (i.e., cold, dry and windy winters) and DSWC and OSC extends all the way down to the basin (Béthoux et al., 2002; Puig et al., 2013). The interplay between both types of water masses has been analyzed in some recent studies (Font et al., 2007; Palanques et al., 2009, 2012; Durrieu de Madron et al., 2013; Puig et al., 2013; Durrieu de Madron et al., 2017), but their effect on the composition of particle fluxes on the basin has not been studied in detail.

Particle fluxes have been recorded in 2005 when both processes reached the basin (Palanques et al., 2009, 2011), in 2007, 2008 without deep dense water formation, and in 2013 when mainly OSC reached the basin seafloor (Stabholz et al., 2013; Houpert et al., 2016; Durrieu de Madron et al., 2017). These studies include some analysis of major components of trapped particles and they basically show an increase of total mass fluxes and lithogenic content and a decrease of biogenic components, especially organic carbon content. These processes also occur in other Mediterranean areas, such as the Southern Adriatic Margin, where the Bari Canyon System can intercept dense waters and sediments and convey this material into the southern Adriatic pit (Trincardi et al., 2007; Turchetto et al., 2007; Rubino et al., 2012)

Winter 2012 can be considered an exceptionally cold and windy year in the northwestern Mediterranean due to the frequent N-NW wind storms with speed $\geq 20\,\mathrm{m\,s^{-1}}$ measured from mid-December 2011 to mid-March 2012. These strong wind events induced a massive formation of dense water on the Gulf of Lions continental shelf and in the open sea region, and both, DSWC and OSC waters reached the basin (Durrieu de Madron et al., 2013). The same winter 2012 cold air outbreak of exceptional intensity also hit the northern Adriatic basin (Mihanović et al., 2013; Davolio et al. (2015) inducing cold and dry northeasterly winds unceasingly blowing during weeks generating dense water masses that migrated southwards along the continental shelf (Langone et al., 2016; Carniel et al., 2016) propagating upwelling and downwelling patterns along broad sectors of the continental slope (Bonaldo et al., 2018).

In the northwestern Mediterranean, Durrieu de Madron et al. (2013) showed a synoptic view of the winter 2012 dense water formation and spreading at a basin scale using data from several deep-sea moorings deployed at different sites of the northwestern Mediterranean, including our study site called "Fondeo Famoso" (FOFA), located at the Catalan continental rise (Fig. 1). The region of intense vertical mixing extended over a large part of the northwestern Mediterranean, forming a chimney about 60 km of radius with the FOFA site being on the periphery. The weakening of the vertical stratification of the "preconditioning phase" and the thickening of the mixed layer started in December 2011 and the newly formed dense water reached the basin seabed on 10 February 2012 inducing an increase in the near-bottom temperature and salinity (Durrieu de Madron et al., 2013). The effects of the homogenization of the water column within the "violent mixing phase" took place from mid-February to late February and the filling of the basin by dense water corresponding with the "sinking and spreading phase" began in early March and extended beyond May and dense shelf water cascading generated temperature drops at the study site from mid-February to early-April (Durrieu de Madron et al., 2013). The objective of this paper is the study of the effects of the DSWC and OSC interaction on the near-bottom trapped particle fluxes and composition and on suspended sediment dynamics at the FOFA site during winter 2012.

2. Methods

The FOFA moored instrumented array was deployed in the Catalan continental rise at 2450 m water depth from November 2011 to July 2012. The array was equipped with 1) a Technicap PPS 3/3-24S cylindrical sediment trap with a $0.125\,\mathrm{m^2}$ collecting area and 24 receiving cups placed 25 m above bottom (mab), 2) a Wetlab ECO fluorometer and a Seapoint turbidimeter installed on a Sea-Bird CTD SBE-16 at 23 mab, and 3) a Nortek Aquadopp current-meter coupled with a Sea-Bird CTD SeaCAT and a Seapoint turbidimeter deployed at 10 mab.

The current meter and CTD sampling intervals were set at 10 min. The sediment trap collecting interval was set at 8 days for most of the 24 samples and at 16 days for the first sample and the last 3 samples. The last sediment trap sample closed in mid-June, before the mooring recovery. Sediment trap cups were filled with a borax-buffered 5% formaldehyde solution in 0.20-μm filtered sea water before their deployment, to prevent sample degradation. After the trap recovery, pH was measured in each cup to check that there was no acidification on any of them. Trapped material was split with a peristaltic dispenser to divide the total sample into several homogeneous aliquots. Swimmers (those organisms deemed to have actively entered the trap) were removed from the samples by wet-sieving the sample through a 1 mm nylon mess. Samples were left to settle again (for one to two days), and examined under a magnifying glass to remove the organisms smaller than < 1 mm. Subsequently, the samples were washed with very cold Milli-Q water and centrifuged three times to extract all the remaining seawater. Finally, samples were freeze-dried by lyophilisation process and weighed. Total Mass Flux (TMF) was computed using the total mass weight, divided by the trap collecting area ($0.125\,\mathrm{m^2}$) and the sampling interval (in days).

According to the results obtained by Baker et al. (1988) trapping efficiency of cylindrical traps strongly decreases with currents exceeding $12\,\mathrm{cm\,s^{-1}}$. Gardner et al. (1997) suggested that the flux measured by cylindrical traps have little dependence on trap Reynolds numbers over the range from 3500 to 43,000 for the traps they used (diameter = 30.5 cm) that corresponded to an upper velocity of $22\,\mathrm{cm\,s^{-1}}$. Heussner et al. (2006) also estimated that there was not bias for the same kind of sediment traps used in this study, with mean Reynolds numbers varying between 3000 and 40,000 (corresponding to current intensity of 1 and $13\,\mathrm{cm\,s^{-1}}$ respectively). Therefore, considering the maximum near-bottom velocities recorded at the FOFA site, the sediment trap was probably affected by bias during high current events and reported fluxes should be considered as semi-quantitative values.

Organic Carbon (OC) and nitrogen (N) contents of the trapped particles were analyzed in 25% HCl treated and non-treated samples, using an elemental analyzer (EA Flash series 1112) with uncertainties lower than 0.1% as determined from replicates of the certified estuarine sediment MESS-1. Inorganic carbon was then calculated as the difference between total and OC. The stable isotopic composition of OC ($\delta^{13}C_{OC}$) and TN ($\delta^{15}N$) were measured with the elemental analyzer coupled to a Delta C mass spectrometer with a CONFLO III interphase with uncertainties lower than 0.2% as determined from routine replicate measurements of the IAEA reference sample CH-3. Calcium carbonate content was calculated from inorganic carbon using the molecular mass ratio 8.33, assuming that all inorganic carbon was in the form of calcium carbonate.

Biogenic silica was analyzed using a wet-alkaline extraction with sodium carbonate using the method described by Mortlock and Froelich (1989). Finally, the lithogenic fraction was obtained as the difference between the total mass and the rest of the main components (i.e. opal + organic matter + carbonates). Trapped fluxes of the main components have been obtained by multiplying their percentage contents times total mass flux.

The amount of trapped particulate matter collected in the first 10 samples between 1 November and 5 February was lower than 40 mg, which allowed estimating TMF, but there was not enough material for performing all analyses. Thus, samples 2 and 3, samples 4, 5, 6 and 7 and samples 9 and 10 were merged for analyzing C, N, $CaCO_3$, $\delta^{13}C_{OC}$ and $\delta^{15}N$, therefore increasing the sampling intervals for these parameters during certain periods. In addition, there was not enough material for analyzing opal (and subsequently lithogenics content) on these first 10 samples.

To have a better constrain on the DSWC period, the data collected at the FOFA mooring site has been compared with near-bottom currents, temperature and turbidity time series collected at 300 m depth at the Cap de Creus Canyon (CCC) head. These time series were recorded by means of an Aanderaa current meter equipped with a 0–25 FTU and a 0–500 FTU turbidity sensor, programmed with a sampling interval of 30 min. This shallower mooring site has been collecting data since 2003, as part of the HydroChanges network (Schroeder et al., 2013), providing a continuous assessment of the interannual variability of DSWC events on the northwestern Mediterranean.

Since no repeated water samples could be collected at the mooring sites for calibration purposes, turbidity values, recorded in FTU (Formalin Turbidity Unit), were converted into estimates of suspended sediment concentration (SSC), following the general calibration curves for the northwestern Mediterranean presented in Guillén et al. (2000):

(1) For FTU > 0.2: SSC = 1.74 FTU − 1.32 (N = 133, $r^2 = 0.99$).

(2) For FTU < 0.2: SSC = 0.79 FTU + 0.18 (N = 159, $r^2 = 0.61$).

Similarly, fluorescence readings were not calibrated with microalgae commonly found at the study site, and chlorophyll-a (Chl-a) values have been obtained from the correlation provided by the sensor manufacturer. Therefore, reported values from the time series should be

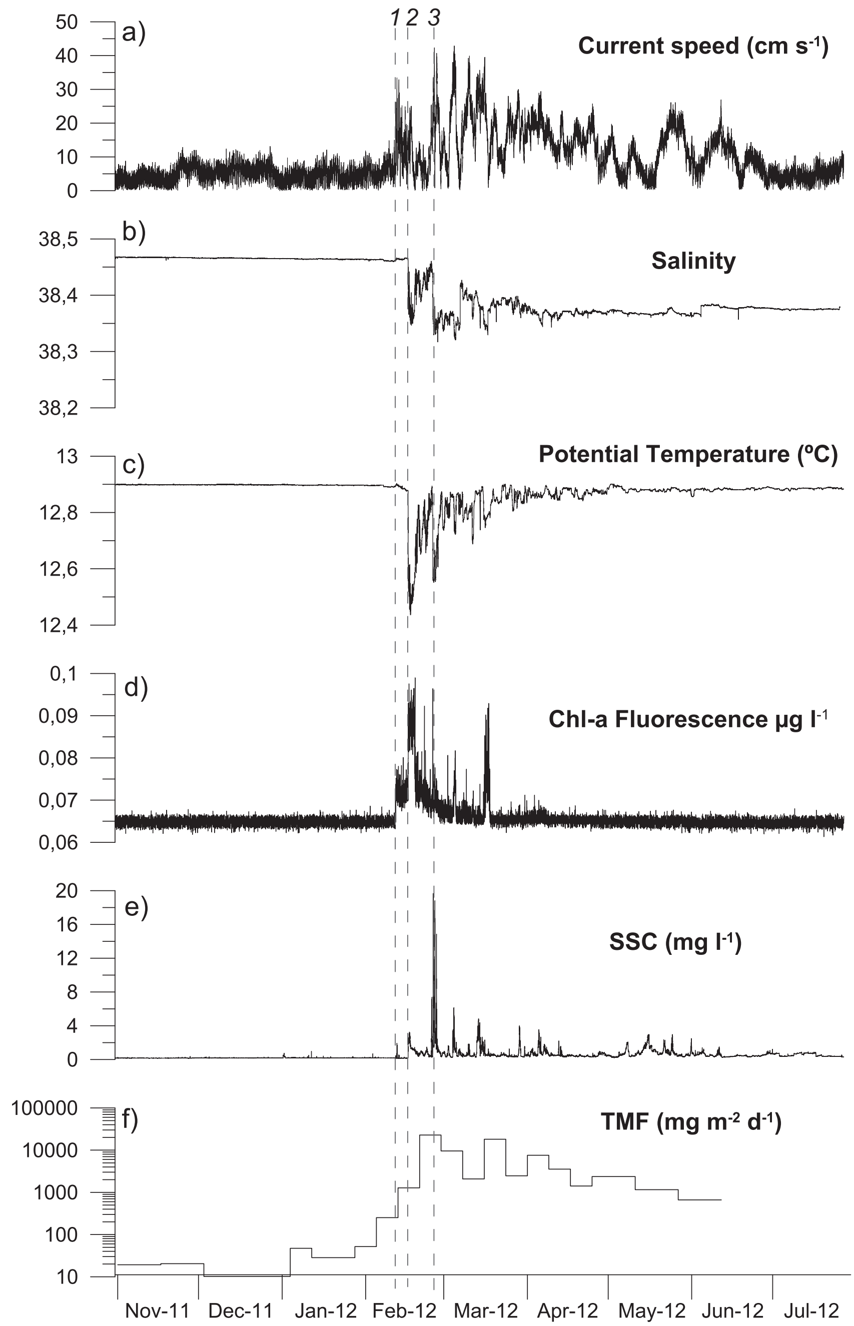

Fig. 2. Time series of a) current speed, b) salinity, c) potential temperature, d) fluorescence, e) suspended sediment concentration (SSC) and f) trapped total mass flux (TMF) recorded at the FOFA site (location in Fig. 1) from November 2011 to July 2012. Numbers 1–3 and thick dashed lines represent the main events described in the Results section.

considered estimates of SSC and Chl-a fluorescence, aimed to visualize the temporal evolution of these parameter throughout the deployment period.

Instantaneous sediment fluxes at the FOFA site were obtained by multiplying the current speed by the SSC at each location.

3. Results

3.1. Hydrographic and total mass fluxes time series

Hydrographic parameters and trapped TMF recorded at the FOFA site during autumn 2011 and winter and spring 2012 showed relatively steady values from November to mid-February, a strong variability from mid-February to early April and progressively more attenuated variability from then to the end of the deployment (Fig. 2).

From November 2011 to mid-February 2012, current velocities ranged mainly between 1 and 10 cm s^{-1} (Fig. 2a), salinity and temperature maintained quite steady values (about 38.45 and 12.9 °C respectively) (Fig. 2b, c) with very low Chl-a fluorescence (0.063 µg l^{-1}), SSC (< 0.1 mg l^{-1}) and TMF (10–50 mg m^{-2} d^{-1}) (Fig. 2d–f). No significant events, from the hydrographic point of view, could be highlighted during this period.

From mid-February, to April, the current velocity, Chl-a fluorescence, SSC and TMF showed large variability that indicated the occurrence of three main events. The first one occurred on February 12th and generated an important increase of the current speed (up to

26 cm s^{-1}) with a slight increase of Chl-a fluorescence values (up to ~0.074 μg l^{-1}) (Fig. 2a, d). During the following four days, current velocity peaks up to 32 cm s^{-1} occurred along with a small increase of the TMF (to 250 mg m^{-2} d^{-1}). A second event occurred on 16 and 17 February, when temperature and salinity decreased down to 12.45 °C and to 38.30 respectively (Fig. 2b, c), at the same time that Chl-a fluorescence and SSC values increased up to 0.097 μg l^{-1} and 3.12 mg l^{-1}, respectively (Fig. 2d, e). A third event took place between 25 and 27 February 2012, which generated a second temperature and a salinity drop down to 12.56 °C and 38.28, respectively (Fig. 2a,b) and subsequent current speed increases between 30 and 40 cm s^{-1} associated with SSC peaks between 7 and 19 mg l^{-1} that lasted from 6 to 10 h (Fig. 2a, e). In addition, during this third event the TMF reached the maximum recorded value of 22,878 mg m^{-2} d^{-1} (Fig. 2f).

From late February to mid-March, there were weaker episodes of decreasing temperature and salinity (Fig. 2b, c) with current increases above 30 cm s^{-1} and some SSC and Chl-a fluorescence peaks up to 6 mg l^{-1} and 0.081 μg l^{-1}, respectively, not always concurrent among them (Fig. 2a, d,e). These peaks last from 9 to 30 h. After mid-March, an important TMF increase (18,157 mg m^{-2} d^{-1}) occurred during a period with low current velocities (< 20 cm s^{-1}) and SSC values (< 2 mg l^{-1}) with some Chl-a fluorescence peaks (up to 0.092 μg l^{-1}) (Fig. 2a, f).

In April, the intensity of the temperature drops decreased and by the end of the month they became unnoticeable. From May to mid-June, there were still some current velocity increases > 20 cm s^{-1} and several SSC peaks of up to 3 mg l^{-1} lasting between 6 and 14 h (Fig. 2a, c, d, e). Many of these SSC peaks recorded in May and June were not correlated with high current speeds. During this period, Chl-a fluorescence was low and TMF progressively decreased with time (Fig. 2f).

3.2. Composition of the trapped particulate matter

Contents and fluxes of the major components of the trapped particulate matter, along with OC:N ratios and the isotopic composition of OC and TN are shown in Fig. 3. In general, there was a strong contrast between the composition of the trapped particulate matter collected in December and January and the one collected from March to June.

Between December and mid-February, trapped particulate matter showed high OC (7.4–10%), $CaCO_3$ (30–50%), TN (0.56–1.46%) and $\delta^{13}C_{OC}$ (−24.0 – −22.0) values and low $\delta^{15}N$ (−2.8–0.6) and OC:N (5.9–8.0) values. In late February, during the three major events, there were strong fluctuations in particle composition, showing a decrease of OC, Opal, TN, and $\delta^{13}C_{OC}$ values and an increase of lithogenics, OC:N and $\delta^{15}N$. Event 3 generated the maximum TMF, and the maximum OC, opal, $CaCO_3$ and lithogenic fluxes (Fig. 3). Between March and June, low Opal (3–4%), TN (0.11–0.17), OC:N (7.7–11.4) and $\delta^{13}C_{OC}$ (−28.2 – −25.2) values – and high $\delta^{15}N$ (1.1–2.3) values were observed.

4. Discussion

4.1. Interactions of OSC, DSWC and particulate matter

This study shows the effects of the deep dense water formation during winter 2012, both by deep OSC and DSWC, on the hydrography, hydrodynamics and particle fluxes and composition in the northwestern Mediterranean basin. The three phases of the OSC taking place in 2012 could be identified in the time series, in concordance with the analysis conducted by Durrieu de Madron et al. (2013): 1) the weakening of the vertical stratification of the "preconditioning phase" from December to mid-February; 2) the homogenization of the water column during the "violent mixing phase" from mid-February to late February, which includes the three main events described in the Results section; and 3) the filling of the basin by the newly formed dense water during the "sinking and spreading phase" from early March to mid-June (Figs. 2 and 4).

During preconditioning phase, hydrological conditions at the FOFA site were relatively steady with low suspended particles concentration and trapped particle fluxes (Figs. 2 and 4). Before the start of the violent mixing phase, DSWC began to reach the CCC head at 300 m depth on January 26, when temperature dropped from 13.46 to 12.46, current speed increased up to 100 cm s^{-1} and estimates of SSC increased to > 10 mg l^{-1}, reaching up to 38 mg l^{-1} on January 31 (Fig. 4). DSWC progressively affected deeper parts of the margin, reaching 1000 m water depth at the CCC axis on February 5 (Durrieu de Madron et al., 2013) and arriving at the FOFA site, (2450 m water depth)on February 16 (event 2), 20 days later than the first CCC observations at 300 m water depth (Figs. 4 and 5).

Previously, OSC reached the FOFA site on February 12 (event 1), four days earlier than the DSWC (Figs. 4 and 5). This first arrival of newly formed dense water by OSC barely changed the ambient temperature and salinity, but increased current velocities and Chl-a fluorescence values (Fig. 5). SSC did not increase until the arrival of the first DSWC pulse on February 16 (event 2), which also caused a strong temperature drop and increases of current velocity, fluorescence and trapped TMF (Figs. 4 and 5). The fact that both SSC and Chl-a fluorescence values increased at the same time suggests that this pulse resuspended and advected recently deposited and easily erodible particles that reached the basin seafloor.

A second major DSWC pulse (event 3) arrived at the FOFA site on February 25, at the end of the violent mixing phase, generating high current speeds concurrent with strong SSC peaks (Figs. 2, 3 and 5). The very high estimated SSC values (up to 19 mg l^{-1}) recorded during this event might suggest that this second DSWC pulse not only caused local resuspension of deep sea sediments, but also delivered resuspended particles advected from the continental slope region perhaps related to the SSC increase at the CCC head in late January, which could have concurrently occurred in other canyon heads (Palanques et al., 2006). These particles could have been transported to the deeper parts of the slope and towards the basin by consecutive resuspension and cascading pulses, as observed during the major DSWC from winter 2006 (Palanques et al., 2012).

During the "sinking and spreading phase" maximum current velocity peaks of up to 40 cm s^{-1} occurred at the FOFA site until mid-March, but although they were similar to those of the violent mixing phase, they produced smaller SSC peaks (Fig. 5). DSWC ended in early April at CCC 300 and became very weak at the FOFA site after late March. Maximum current velocities decreased from late March to mid-June. However, some current speed peaks reaching up to 30 cm s^{-1} and several SSC peaks of up to 3 mg l^{-1} were still recorded (Figs. 2 and 4). Some of these SSC peaks could be still linked to sediment resuspension during current speed increases, but many of them occurred with low currents (< 10 cm s^{-1}), presumably as advected suspended particle clouds.

The current peaks matching the arrival of the OSC and from the beginning of the violent mixing phase to the end of the sinking and spreading phase (Fig. 2a) are presumably associated with the development of deep eddies (both anticyclonic and cyclonic) that drifted far away from the deep convection area (Testor and Gascard, 2006; Houpert et al., 2016). The maximum currents recorded at the FOFA site were similar to those recorded at the center of the OSC region (LION site; 5° E 42° N) in 2012 (Durrieu de Madron et al., 2013). These maximum currents were also similar to the ones recorded at the center of the OSC region in 2010, 2011 and 2013, when only deep OSC reached the basin (Durrieu de Madron et al., 2017). This suggests that DSWC barely contributes to the generation of such strong currents affecting the northwestern Mediterranean basin and that they are mainly induced by OSC.

In contrast, the SSC peaks recorded at the FOFA site during 2012 were up to one order of magnitude higher than those recorded at the center of the OSC region (LION site) (Durrieu de Madron et al., 2017), in spite of the similar maximum currents recorded at both zones. At the same time, temperature drops recorded at the FOFA site (0.5 °C cooling on February 16) were stronger and occurred much earlier than those

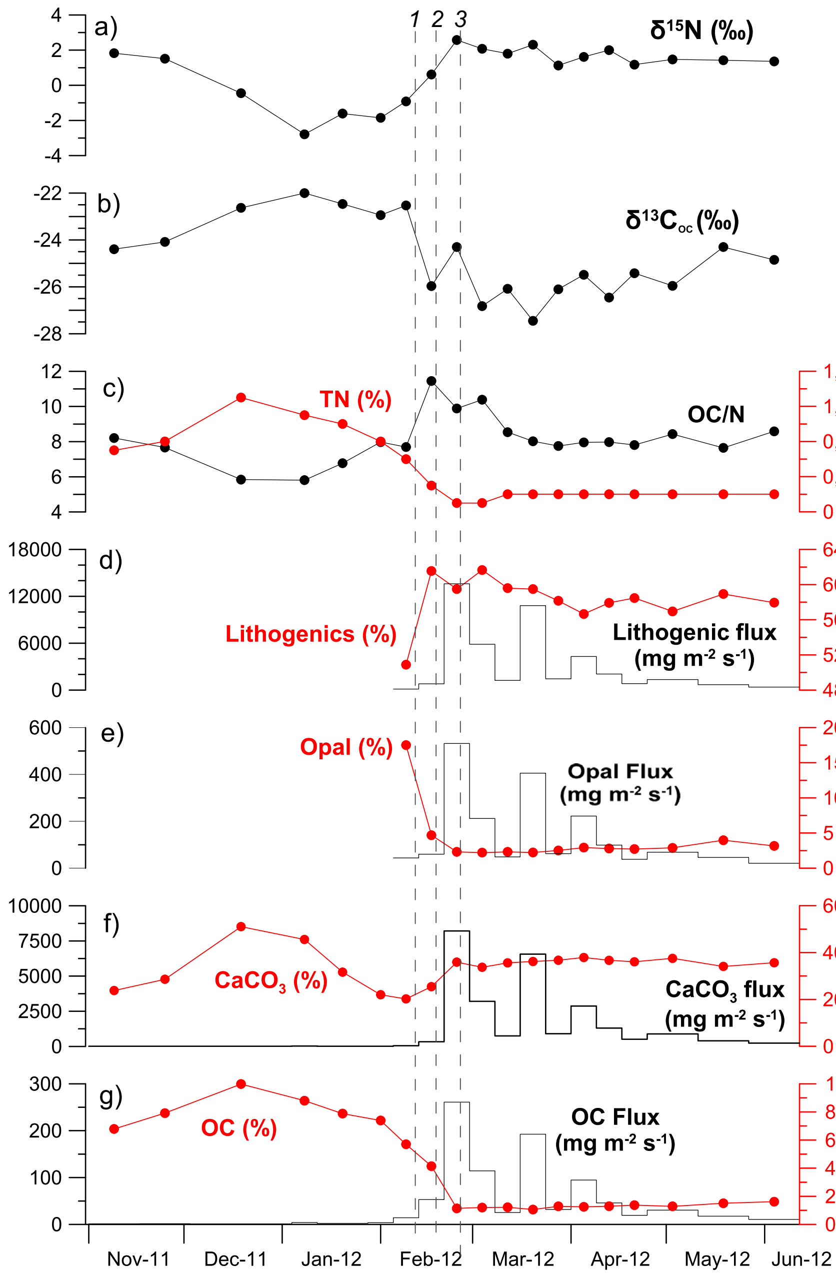

Fig. 3. Time series of a) $\delta^{15}N$, b) $\delta^{13}C_{OC}$, c) OC/N (molar) and total nitrogen (TN), d) lithogenics flux and content, e) opal flux and content, f) $CaCO_3$ flux and content and g) OC flux and content of the particulate matter trapped at the FOFA site (location in Fig. 1) from November 2011 to July 2012. Numbers 1–3 and thick dashed lines represent the main events described in the Results section. As there was not enough trapped material for performing all analyses in the first 10 samples, samples 2 and 3, samples 4, 5, 6 and 7 and samples 9 and 10 were merged for analyzing C, N, CaCO3, δ13COC and δ15N increasing the sampling intervals. There was not enough material for analyzing opal and lithogenics content on these first 10 samples.

recorded at the center of the OSC region (0.1 °C cooling on March 1; Durrieu de Madron et al., 2013). This means that the FOFA site, being located at the north Catalan continental rise, received a higher influence of the DSWC water and sediment load than the LION site. In fact, SSC peaks generated at the center of the OSC zone site in 2010, 2011 and 2013 with only deep OSC were similar to those generated in 2012 with both deep OSC and DSWC (Durrieu de Madron et al., 2017), indicating that the influence of DSWC sediment load in this zone is low.

These findings suggest that the deep DSWC plume and its sediment load affect mainly the Catalan margin and flows along the continental rise as a contour current. This agrees with the observations made in 2006, when deep DSWC pulses overflowed the CCC between 1000 and 1500 m depth with a dominant along slope component towards the south of the CCC (Palanques et al., 2012).

4.2. Benthic storms caused by deep dense water formation

Oceanographic processes able to exceed the critical bed shear stress and cause sediment resuspension on deep oceanic regions are poorly known. Large, episodic increases in bottom-water turbidity in the deep ocean were first documented on the northwestern Bermuda Rise in the Western North Atlantic (Gardner and Sullivan, 1981), where the term “benthic storms” was initially coined. Later, similar events were intensely studied on the lower continental rise south of Nova Scotia during the HEBBLE Project (Hollister and McCave, 1984; Pak, 1983; Pak and Zaneveld, 1983; Grant et al., 1985; Gardner et al., 1985; Hollister and Nowell, 1991). Benthic storms were also studied on the lowermost continental rise and Hatteras Abyssal Plain off the eastern United States (Isley et al., 1990), in the northeast Atlantic (Klein and Mittelstaedt, 1992), and in the Argentine Basin (Richardson et al., 1993). These benthic storms were generally coincident with current speeds in excess of ~20 cm s^{-1} and they generated pronounced increases in the SSC of the bottom nepheloid layer. Although the origin of these events was not well identified, the accepted hypothesis was that they could be generated by topographic waves excited by Gulf Stream oscillations (Hollister and Nowell, 1991). In fact, Heezen and Hollister

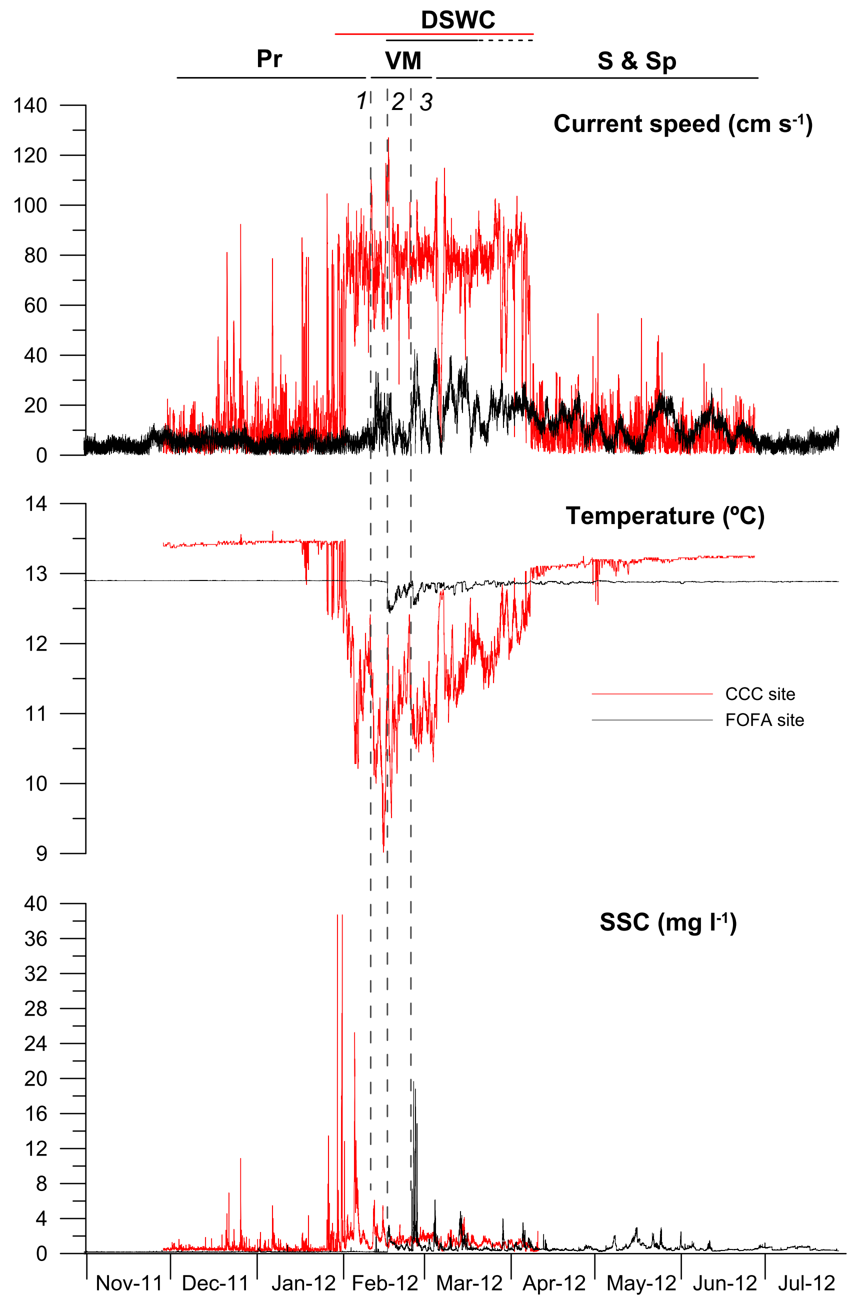

Fig. 4. Time series of current speed, temperature and suspended sediment concentration (SSC) recorded at the CCC (red lines) and the FOFA sites (black lines) from November 2011 to July 2012 (see location in Fig. 1). Numbers 1–3 and thick dashed lines represent the main identified events: 1: Arrival of the OSC; 2: first DSWC pulse; 3: second DSWC pulse at the FOFA site. *Pr*: Preconditioning phase; VM: violent mixing phase; Sp: Spreading and mixing phase; DSWC: dense shelf water cascading at the CCC site in red and at the FOFA site in black (Discontinuous line indicates weakening of DSWC at the FOFA site).

(1972) had previously suggested that perturbations from deep eddy-type flows could affect seafloor erosion, suspension, and advection of sediment. This pattern has been supported later by models and currents measurements (Arbic et al., 2009, 2010; Wright et al., 2013).

Recently, Gardner et al. (2017) analyzed and reviewed these events comparing benthic storms to dust storms in that the fluid (air/water) moves fast enough to erode and resuspend the underlying sediment, mixing it with the overlying fluid to create clouds of dust/particulate matter that are redistributed downwind/downstream. They also pointed out that benthic storms on the western North Atlantic often closely match the position of Gulf Stream meanders and rings, which energy is propagated downward, sometimes reaching the seafloor in the form of cyclones, anticyclones, or topographic waves, generating current speeds sufficient to resuspend and erode surface sediments. They also observed some high SSC correlated with low current speeds indicating either advection from a distal event or slowing of currents following a local event and referred to these occurrences as "storm tails".

The records at the FOFA site, suggests that several of the observed events causing high currents and increases in SSC could be defined as benthic storms, as well, but produced mainly by bottom-reaching dense water formation and the associated deep eddy activity. These benthic storms are generated mainly by deep OSC that induce sediment resuspension and advection and can be feed and enhanced by the sediment load supplied by concurrent deep DSWC pulses. Accordingly, benthic storms resuspending bottom sediment could be observed mainly from mid-February to mid-April during part of the violent mixing and the sinking and spreading phases, including the two pulses

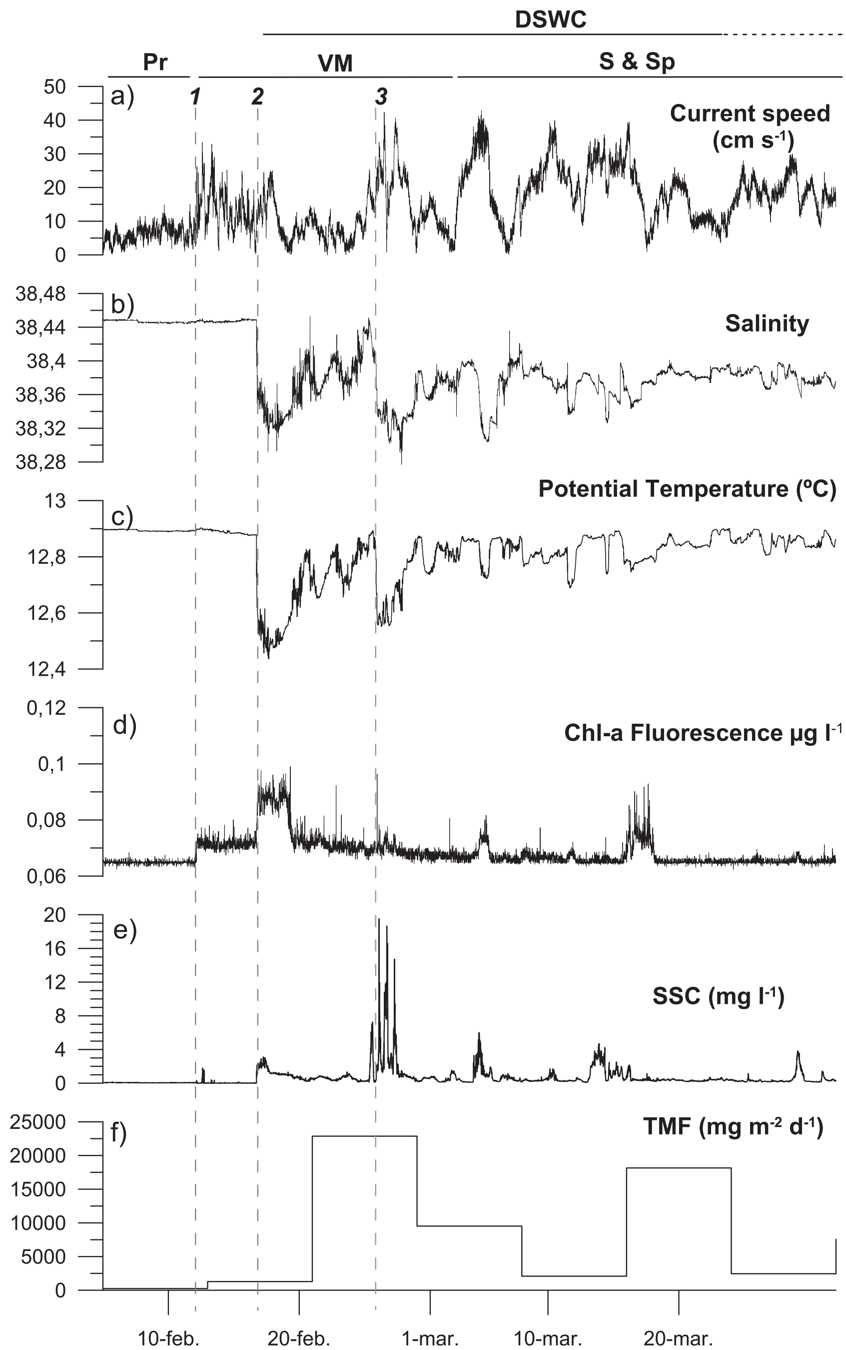

Fig. 5. Zoom of time series of a) current speed, b) salinity, c) potential temperature, d) fluorescence, e) suspended sediment concentration (SSC) and f) trapped total mass flux (TMF) recorded at the FOFA site (location in Fig. 1) from 5 February 2012 to 1 April 2012. Numbers 1–3 and thick dashed lines represent: 1: Reaching of the OSC at the FOFA site; 2: first DSWC pulse; 3: second DSWC pulse. In the top, Pr: Preconditioning phase; VM: violent mixing phase; Sp: Spreading and mixing phase. DSWC: dense shelf water cascading at the FOFA site (Discontinuous line indicates weakening of DSWC).

of deep DSWC, and storm tails arrived at the mooring site during periods of low currents in May and early-June, at the end of the sinking and spreading phase. Suspended sediment fluxes during benthic storms ranged between 500 and 6500 mg m^{-2} d^{-1}, which are increases between 1 and 2 orders of magnitude, whereas they ranged between 100 and 250 mg m^{-2} d^{-1} during storm tails (Fig. 6).

These storm tails would correspond to suspended matter clouds advected by the OSC-induced eddies distributed all over the basin after the most energetic period. This particulate matter remained in suspension for months and contributed to form the thick BNL that develops in the deep basin each time that major deep DSWC and OSC events occur (Puig et al., 2013; Durrieu de Madron et al., 2017). This thick massive BNL is several hundred meters thick (around 2000 m in the center of the convection region) and can last from some months up to several years.

Recent near-bottom mooring observations in the northwestern Mediterranean basin suggest that similar resuspension events attributable to benthic storms might have occurred in previous years. In 2005, recorded at the EFLUBIO mooring site (Palanques et al., 2009, 2011); in 2006, observed both in the northern Catalan continental rise (Palanques et al., 2012) and in the Ligurian Sea basin (Martín et al., 2010); in 2009 at the FAMOSO and ICM-Hydrochanges mooring sites (Salat et al., 2010; Puig et al., 2012) and in 2010, 2011, 2012 and 2013 at the LION mooring site (Durrieu de Madron et al., 2017). All of them

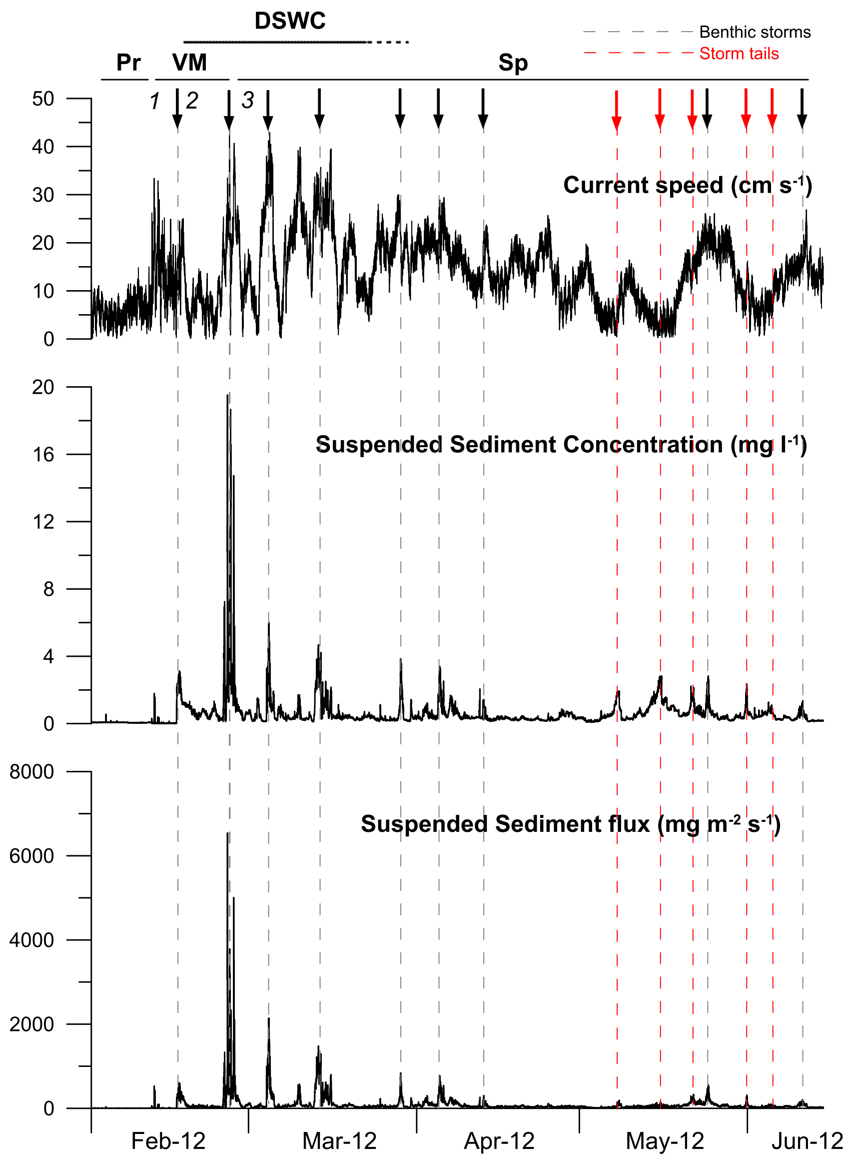

Fig. 6. Time series of current speed suspended sediment concentration and suspended sediment flux recorded at the FOFA site (location in Fig. 1) from November 2011 to June 2012. Arrows and discontinuous vertical lines correspond with significant SSC peaks that can be defined as benthic storms (black) and storm tails (red). Labels as defined in Fig. 5 caption.

occurring during deep OSC events, and those from 2005, 2006 and 2012 also concurrent with deep DSWC, reaching the basin seafloor.

The benthic storms generated by OSC and DSWC observed up to now in the NW Mediterranean at 2450 m depth with currents between 30 and 40 cm s^{-1} generate trapped particle fluxes up to 23,000 mg m^{-2} d^{-1}. Similar benthic storms could also be generated in other Mediterranean regions. Langone et al. (2016) recorded exceptional trapped particle fux increases of up to 14,860 mg m^{-2} d^{-1} in the Southern Adriatic from March to June in 2012 during the strong DSWC period that also affected that area. Temperature records showed in their study suggest that probably deep OSC also occurred in this area at the same time and perhaps similar benthic storms could have also been generated in the Southern Adriatic.

To put these Mediterranean TMF fluxes generated by benthic storms during DSWC and OSC into context, benthic storms associated with Gulf Stream meanders and rings at 5022 m depth in the Nova Scotian Rise with mean current speed of 32 cm s^{-1}generate trapped particle fluxes of up to 77,000 mg m^{-2} d^{-1} (Gardner et al., 1983).

4.3. Effects of the dense water formation processes in the particulate matter composition

Although both deep OSC and DSWC increase near-bottom currents that can resuspend and transport particulate matter, particles can come from different sources and with different compositions. The particle OC sources can be identified by the stable carbon isotopic composition of the organic matter collected in the sediment trap samples. Temperate marine plankton has $\delta^{13}C_{OC}$ values ranging from −22 to −19‰ (Fry and Sherr, 1984), whereas fluvial particulate organic matter is a function of contributions mainly from freshwater phytoplankton with $\delta^{13}C_{OC}$ values of −30 to −25‰ and particulate terrestrial organic matter with $\delta^{13}C_{OC}$ values of −25 to −33‰ (Salomon and Mook, 1981; Middelburg and Nieuwenhuize, 1998). In general, in the FOFA sediment trap samples there is always a mixture of terrestrial and marine inputs with their proportion changing with time. A simple $\delta^{13}C_{OC}$–based binary mixing model assuming an average marine $\delta^{13}C_{OC}$ of −21‰ and terrestrial $\delta^{13}C_{OC}$ = −27‰ endmembers was made to evaluate the contribution of the marine and terrestrial sources as inputs of organic matter (OM) at the FOFA mooring site. This approach shows

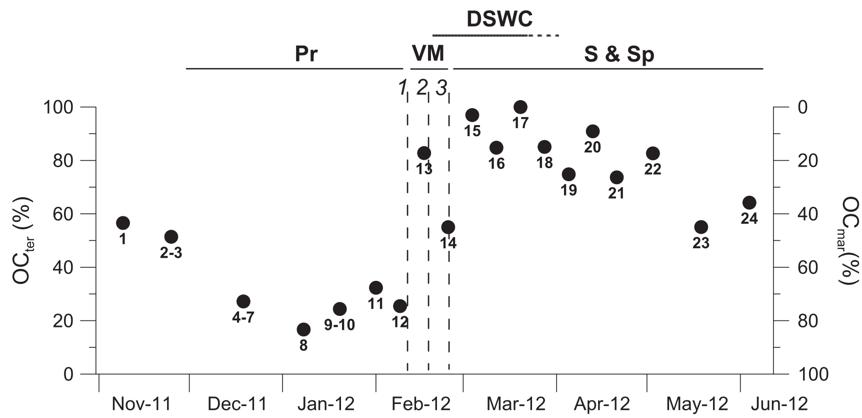

Fig. 7. Plot showing the temporal evolution of terrestrial (left axis) and marine (right axis) organic matter at the FOFA site obtained following a mixing model. Labels as defined in Fig. 5 caption.

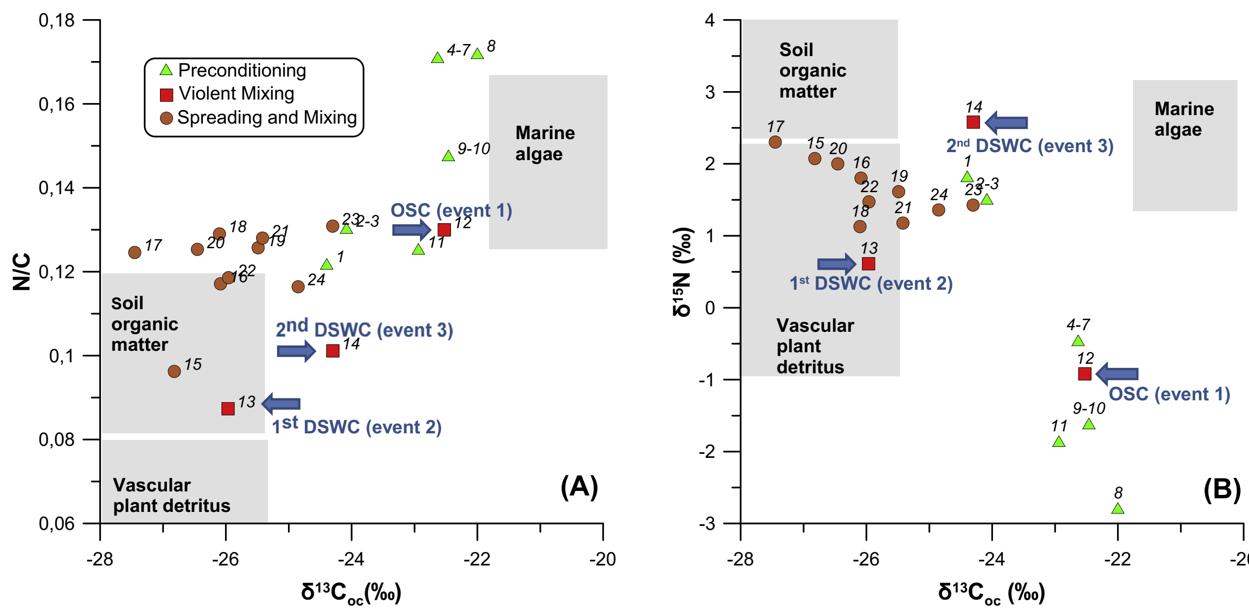

Fig. 8. (A) Plot of $\delta^{13}C_{OC}$ vs. N:C atomic ratio of trapped particles along with potential sources (marine algae, C3 soil organic matter, and vascular plant detritus). Compositional range of values from Meyers (1994), Goñi and Hedges (1995), Hedges et al. (1997), Goñi et al., 2008. (B) Plot of $\delta^{13}C_{OC}$ vs. $\delta^{15}N$ of trapped particles during the different OSC phases (Preconditioning phase, violent mixing phase and Spreading and mixing phase), along with potential sources. Samples Compositional range of values from Altabet (1996) and Amundson et al. (2003). OSC: Reaching of the OSC at the FOFA site; 1st DSWC: first DSWC episode; 2nd DSWC: second DSWC episode. Sample numbers correspond to samples labeled in Fig. 7. Deep DSWC occurred from sample 13 to 18.

a dominant marine source in December and January, an abrupt change from marine to terrestrial sources during the violent mixing phase and the major deep DSWC pulses and a gradual change from terrestrial to less terrestrial sources during the sinking and spreading phase (Fig. 7). Application on stable carbon isotopes in source studies, however, includes uncertainty on several levels that can be reduced applying a second measurement as OC/N. Generally, higher OC/N ratios at more negative $\delta^{13}C_{OC}$ values can indicate increased percentages of riverine material (Kennicutt et al., 1987), a wide OC/N ratio range of 15–30 indicate "terrestrial" material with $\delta^{13}C_{OC}$ values near −28‰, whereas OC/N values of about 7 indicate marine plankton (Hedges et al., 1986). Thus, the source of the OM in the trapped particles of the FOFA site is represented by plotting $\delta^{13}C_{OC}$ against N:C and $\delta^{15}N$ (Fig. 8). N:C is plotted instead of C:N because the former allows direct comparison with other carbon normalized parameters (i.e., ^{13}C:^{12}C) as indicators of carbon sources (Perdue and Koprivnjak, 2007).

During the preconditioning phase, there was first a mixture of marine and terrestrial OC in November and later a dominant input of undegraded OC of marine origin from December to mid-February (Figs. 7 and 8). At the beginning the violent mixing phase (event 1), there was a small increase of the OC flux mainly of marine origin (Figs. 3 and 8), which was probably injected by the first OSC pulse that reached the FOFA site. Later, during this phase, the particles transported by the first DSWC pulse (event 2) had a dominant contribution of terrestrial and probably more degraded OM (Figs. 3b, c and 8A) that could correspond to the more erodible surface sediment from the shelf and slope which arrived with this first pulse added to the deep sediment resuspended by the OSC-induced benthic storm. The increased fluorescence during this DSWC pulse (Fig. 5d) could indicate the sinking of phytoplankton cells and their mixing with the dominant terrestrial OM. Widespread phytoplankton blooms occur often from the end of February (Fabres et al., 2008) and newly produced particles could be transported to the basin mixed with resuspended sediment by sinking dense water both by DSWC and OSC. At the end of the violent mixing phase, the second major DSWC pulse (event 3) supplied a mixture of marine and terrestrial OM less undegraded than that of the previous pulse (Figs. 7 and 8) and generated the maximum trapped TMF and the maximum fluxes of all the analyzed components (Figs. 2 and 3). This pulse could incorporate resuspended sediment and relatively undegraded OM advected both from the shelf and continental slope region by DSWC and deep sediment resuspended by OSC-induced benthic storms with more degraded OM.

During the sinking and spreading phase, there was mainly a dominant contribution of terrestrial and relatively undegraded OM (Figs. 7 and 8) and lower OC contents (1.1–1.6%) (Fig. 3). A particular event took place in mid-March when there was an important flux increase of all the components of the trapped particle matter and of Chl-a fluorescence coinciding with the weakening of the DSWC and with the decrease of maximum currents occurring at that time (Figs. 3 and 6), which could have favored an increased settling of previously suspended particles (Fig. 2).

At the beginning of the sinking and spreading phase, still with presence of DSWC, the OM was mainly terrigenous. However, it became progressively less terrigenous after the end of the deep DSWC, being a mixture of marine and terrestrial OM at the end of this phase (Fig. 7). The period of the more terrestrial OM corresponded with direct resuspension by benthic storms, whereas the less terrestrial period in May and June corresponded mainly with the arrival of storm tails (Fig. 6). This was also correlated with a progressive decrease of the TMF.

Summarizing the general trends, there was a dominant input of undegraded marine OM during the preconditioning and the beginning of the violent mixing phases and an abrupt change to a dominant terrestrial OM mainly during the mid and last part of the violent mixing phase and the first part of the sinking and spreading phase, coinciding with the occurrence of OSC-induced benthic storms. This trend differs from that recorded in year 2006 at 1900 m water depth in the lower CCC area (Sanchez-Vidal et al., 2009), where after the deep DSWC and with OSC, OM became more marine than at the one recorded at the FOFA site. In the same way, data recorded from March to June 2012 in the western margin of the Southern Adriatic also showed a higher contribution of organic carbon of marine origin during DSWC events (Langone et al., 2016) This discrepancy could be perhaps because the deep CCC region in year 2006 and the Southern Adriatic area in year 2012 received more inputs from the concurrent spring blooms and were less affected by the resuspension of the OSC-DSWC induced benthic storms.

During the 24 days of violent mixing phase including the two main DSWC pulses, the mean flux and the total amount of trapped OC ($109.4\ mg\ m^{-2}\ d^{-1}$; $2625.0\ mg\ m^{-2}$) was more than one order of magnitude higher than during the 64 days of the preconditioning phase ($3.6\ mg\ m^{-2}\ d^{-1}$; $230.0\ mg\ m^{-2}$). During the 104 days of sinking and spreading phase the mean OC flux ($49.3\ mg\ m^{-2}\ d^{-1}$) was half of that during the violent mixing phase, but the total amount of relatively undegraded OC ($5127.3\ mg\ m^{-2}$) was double. Although it was mainly terrestrial OM, small fluorescence peaks until late march suggest that fresh marine OM reached the study site but their indicators were masked by the dominant terrigenous inputs.

The increase of the OC flux with relatively undegraded OM during the violent mixing and the sinking and spreading phases contributed to the "fertilization" of the deep pelagic and benthic ecosystems. Fertilization of the basin by previous deep dense water formation events was suggested by Canals et al. (2006), Company et al. (2008), Tamburini et al. (2013), Severin et al. (2014) and Martini et al. (2014), although the exact timing and the evolution of the OM composition could not be elucidated until now.

5. Conclusions

Deep dense water formation increased deep near-bottom currents, fluorescence, suspended sediment concentration, suspended sediment fluxes and trapped particle fluxes at the deep Catalan margin. The high deep currents generated benthic storms that resuspended bottom sediment and redistributed it along the deep slope. Major SSC peaks last between 6 and 30 h. The arrival of the OSC at the FOFA site increased the trapped flux of newly produced marine particles, whereas DSWC first supplied easily erodible material with terrestrial OM and afterwards resuspended and transported large amounts of particulate matter with a mixture of marine and terrestrial OM. During most of the violent mixing phase and the first part of the sinking and spreading phase, which included the DSWC period, there was a dominant input of terrestrial OM with SSC peaks generated by benthic storms. However, from the end of the DSWC until the end of the sinking and spreading phase there was a gradual decrease of the terrestrial OM and SSC peaks occurred mainly as advected benthic storm tails.

During the violent mixing and the sinking and spreading phases, deep OSC and DSWC increased trapped particulate OM fluxes by more than one order of magnitude, contributing significantly to the "fertilization" of the deep pelagic and benthic ecosystems. Chl-a Fluorescence increased mainly during the first OSC and DSWC pulses reaching the FOFA site and after the end of the maximum current speeds period in mid-March.

Acknowledgements

We thank Jacobo Martín, Mikel Latasa, Renate Scharek, the UTM technicians and the crew of R/V Garcia del Cid for their help and dedication during the cruises. The EU research project HERMIONE (FP7-ENV-2008-1-226354), and the research project FAMOSO (CTM 2010-11165-E) funded by the Spanish Ministerio de Ciencia e Innovación supported this research. The authors belong to CRG on Littoral and Oceanic Processes, supported by Grant 2017 SGR 863 of the Generalitat de Catalunya. Reviews by anonymous reviewers were greatly appreciated.

References

Altabet, M.A., 1996. Nitrogen and carbon isotopic tracers of the source and transformation of particles in the deep-sea. In: Ittekkot, V., Schäfer, P., Honjo, S., Depetris, P.J. (Eds.), Particle Flux in the Ocean. Wiley, pp. 155–184.
Amundson, R., Austin, A.T., Schuur, E.A.G., Yoo, K., Matzek, V., Kendall, C., Uebersax, A., Brenner, D., Baisden, W.T., 2003. Global patterns of the isotopic composition of soil and plant nitrogen. Glob. Biogeochem. Cycles 17, 1031.
Arbic, B.K., Shriver, J.F., Hogan, P.J., Hurlburt, H.E., McClean, J.L., Metzger, E.J., Scott, R.B., Sen, A., Smedstad, O.M., Wallcraft, A.J., 2009. Estimates of bottom flows and bottom boundary layer dissipation of the oceanic general circulation from global high resolution models. J. Geophys. Res. 114, C02024.
Arbic, B.K., Wallcraft, A.J., Metzger, E.J., 2010. Concurrent simulation of the eddying general circulation and tides in a global ocean model. Ocean Model 32, 175–187.
Baker, E.T., Milburn, H.B., Tennant, D.A., 1988. Field assessment of sediment trap efficiency under varying flow conditions. J. Mar. Res. 46, 573–592.
Béthoux, J.P., Durrieu de Madron, X., Nyffeler, F., Tailliez, D., 2002. Deep water in the western Mediterranean: Peculiar 1999 and 2000 characteristics, shelf formation hypothesis, variability since 1970 and geochemical inferences. J. Mar. Syst. 33–34, 117–131.
Bonaldo, D., Orlić, O., Carniel, S., 2018. Framing continental shelf waves in the southern Adriatic Sea, a further flushing factor beyond dense water cascading. Sci. Rep. 8, 660.
Canals, M., Puig, P., Durrieu de Madron, X., Heussner, S., Palanques, A., Fabres, J., 2006. Flushing submarine canyons. Nature 444, 354–357.
Carniel, S., Bonaldo, D., Benetazzo, A., Bergamasco, A., Boldrin, A., Falcieri, F.M., Sclavo, M., Trincardi, F., Langone, L., 2016. Off-shelf fluxes across the southern Adriatic margin: Factors controlling dense-water-driven transport phenomena. Mar. Geol. 375, 44–63.
Company, J.B., Puig, P., Sardà, F., Palanques, A., Latasa, M., Scharek, R., 2008. Climate influence on deep sea populations. PLoS One 3, e1431.
Davolio, S., Stocchi, P., Benetazzo, A., Bohm, E., Riminucci, F., Ravaioli, M., Li, Xiao-Ming, Carniel, S., 2015. Exceptional Bora outbreak in winter 2012: Validation and analysis of high-resolution atmospheric model simulations in the northern Adriatic area. Dyn. Atmos. Oceans 71, 1–20.
Durrieu de Madron, X., Zervakis, V., Theocharis, A., Georgopoulos, D., 2005. Comments to "Cascades of dense water around the world ocean". Prog. Oceanogr. 64 (1), 83–90.
Durrieu de Madron, X., Houpert, L., Puig, P., Sanchez-Vidal, A., Testor, P., Bosse, A., Estournel, C., Somot, S., Bourrin, F., Bouin, M.N., Beauverger, M., Beguery, L., Calafat, A., Canals, M., Coppola, L., Dausse, D., D'Ortenzio, F., Font, J., Heussner, S., Kunesch, S., Lefevre, D., Le Goff, H., Martín, J., Mortier, L., Palanques, A., Raimbault, P., 2013. Interaction of dense shelf water cascading and open-sea convection in the Northwestern Mediterranean during winter 2012. Geophys. Res. Lett. 40, 1379–1385.
Durrieu de Madron, X., Ramondenc, S., Berline, L., Houpert, L., Bosse, A., Martini, S., Guidi, L., Conan, P., Curtil, C., Delsaut, N., Kunesch, S., Ghiglione, J.F., Marsaleix, P., Pujo-Pay, M., Séverin, T., Testor, P., Tamburini, C., the ANTARES collaboration, 2017. Deep sediment resuspension and thick nepheloid layer generation by open-

ocean convection. J. Geophys. Res. Oceans 122 (3), 2291–2318.
Estournel, C., Marsaleix, P., Auclair, F., Julliand, C., Vehil, R., 2003. Observations and modeling of the winter coastal oceanic circulation in the Gulf of Lion under wind conditions influenced by the continental orography (FETCH experiment). J. Geophys. Res. 108 (C3), 8059.
Fabres, J., Tesic, T., Velez, J., Batista, F., Lee, C., Calafat, A., Heussner, S., Palanques, A., Miserocchic, S., 2008. Seasonal and event controlled export of fresh organic matter from the shelf towards the Gulf of Lions continental slope. Cont. Shelf Res. 28, 1971–1983.
Font, J., Puig, P., Salat, J., Palanques, A., Emelianov, M., 2007. Sequence of hydrographic changes in NW Mediterranean deep water due to the exceptional winter of 2005. Sci. Mar. 71 (2), 339–346.
Fry, B., Sherr, E., 1984. δ13C measurements as indicators of carbon flow in marine and freshwater ecosystems. Contrib. Mar. Sci. 27, 49–63.
Gardner, W.D., Sullivan, L.G., 1981. Benthic storms: temporal variability in a deep ocean nepheloid layer. Science 213, 329–331.
Gardner, W.D., Richardson, M.J., Hinga, K.R., Biscaye, P.E., 1983. Resuspension measured with sediment traps in a high-energy environment. Earth Planet. Sci. Lett. 66, 262–278.
Gardner, W.D., Biscaye, P.E., Zaneveld, J.R.V., Richardson, M.J., 1985. Calibration and comparison of the LDGO nephelometer and the OSU transmissometer on the Nova Scotian rise. Mar. Geol. 66, 323–344.
Gardner, W.D., Biscaye, P.E., Richardson, M.J., 1997. A sediment trap experiment in the Vema Channel to evaluate the effect of horizontal particle fluxes onmeasured vertical fluxes. J. Mar. Res. 55, 995–1028.
Gardner, W.D., Tucholke, B.E., Richardson, M.J., Biscaye, P.E., 2017. Benthic storms, nepheloid layers, and linkage with upper ocean dynamics in the western North Atlantic. Mar. Geol. 385, 304–327.
Goñi, M.A., Hedges, J.I., 1995. Sources and reactivities of marine derived organic matter in coastal sediments as determined by alkaline CuO oxidation. Geochim. Cosmochim. Acta 59, 2965–2981.
Goñi, M.A., Monacci, N., Gisewhite, R., Crockett, J., Nittrouer, C., Ogston, A., Alin, S.R., Aalto, R., 2008. Terrigenous organic matter in sediments from the Fly River delta-clinoform system (Papua New Guinea). J. Geophys. Res. 113, F01S10.
Grant, W.D., Williams III, A.J., Gross, T.F.A., 1985. Description of the bottom boundary layer at the HEBBLE site: low frequency forcing, bottom stress and temperature structure. Mar. Geol. 66, 219–241.
Guillén, J., Palanques, A., Puig, P., Durrieu de Madron, X., Nyffeler, F., 2000. Field calibration of optical sensors for measuring suspended sediment concentration in the Western Mediterranean. Sci. Mar. 64 (4), 427–435.
Hedges, J.I., Clark, W.A., Quay, P.D., Richey, J.E., Devol, A.H., Santos, U.M., 1986. Composition and fluxes of particulate organic material in the Amazon River. Limnol. Oceanogr. 31, 717–738.
Hedges, J.I., Keil, R.G., Benner, R., 1997. What happens to terrestrial organic matter in the ocean? Org. Geochem. 27, 195–212.
Heezen, B.C., Hollister, C.D., 1972. The Face of the Deep. Oxford Univ. Press, New York (659 pp).
Heussner, S., Durrieu De Madron, X., Calafat, A., Canals, M., Carbonne, J., Delsaut, N., Saragoni, G., 2006. Spatial and temporal variability of downward particle fluxeson a continental slope: lessons from an 8-yr experiment in the Gulf of Lions (NW Mediterranean). Mar. Geol. 234, 63–92.
Hollister, C.D., McCave, I.N., 1984. Sedimentation under deep-sea storms. Nature 309, 220–222.
Hollister, C.D., Nowell, A.R.M., 1991. HEBBLE epilogue. Mar. Geol. 99, 445–460.
Houpert, L., Durrieu de Madron, X., Testor, P., Bosse, A., Bouin, M.N., Dausse, D., Le Goff, H., Kunesch, S., Labaste, M., Coppola, L., D'Ortenzio, F., Mortier, L., Raimbault, P., 2016. Observations of open-ocean deep convection in the northwestern Mediterranean Sea: seasonal and interannual variability of mixing and deep water masses for the 2007–2013 period. J. Geophys. Res. Oceans 121, 8139–8171.
Isley, A.E., Pillsbury, R.D., Laine, E.P., 1990. The genesis and character of benthic turbid events, northern Hatteras Abyssal Plain. Deep-Sea Res. 37, 1099–1119.
Kennicutt, M.C., Barker, C., Brooks, J.M., DeFreitas, D.A., Zhu, G.H., 1987. Selected organic matter source indicators in the Orinoco, Nile and Changjiang deltas. Org. Geochem. 11, 41–51.
Killworth, P.D., 1976. The mixing and spreading phases of MEDOC-1. Prog. Oceanogr. 7, 59–90.
Klein, H., Mittelstaedt, E., 1992. Currents and dispersion in the abyssal Northeast Atlantic: results from the NOAMP field program. Deep-Sea Res. 39, 1727–1745.
Langone, L., Conese, I., Miserocchi, S., Boldrin, A., Bonaldo, D., Carniel, S., Chiggiato, J., Turchetto, M., Borghini, M., Tesi, T., 2016. Dynamics of particles along the western margin of the Southern Adriatic: processes involved in transferring particulate matter to the deep basin. Mar. Geol. 375, 28–43.
L'Heveder, B., Li, L., Sevault, F., Somot, S., 2013. Interannual variability of deep convection in the Northwestern Mediterranean simulated with a coupled AORCM. Clim. Dyn. 41, 937–960.
Marshall, J., Schott, F., 1999. Open-ocean convection: observations, theory, and models. Rev. Geophys. 37 (1), 1–64.
Martín, J., Miquel, J.C., Khripounoff, A., 2010. Impact of open sea deep convection on sediment remobilization in the western Mediterranean. Geophys. Res. Lett. 37, L13604.
Martini, S., Nerini, D., Tamburini, C., 2014. Relation between deep bioluminescence and oceanographic variables: a statistical analysis using time–frequency decompositions. Prog. Oceanogr. 127, 117–128.
MEDOC group, 1970. Observation of formation of deep water in the Mediterranean Sea. Nature 227, 1037–1040.
Meyers, P.A., 1994. Preservation of elemental and isotopic source identification of organic matter. Chem. Geol. 144, 289–302.
Middelburg, J.J., Nieuwenhuize, J., 1998. Carbon and nitrogen stable isotopes in suspended matter and sediments from the Schelde Estuary. Mar. Chem. 60, 217–225.
Mihanović, H., Vilibić, I., Carniel, S., Tudor, M., Russo, A., Bergamasco, A., Bubić, N., Ljubešić, Z., Viličić, D., Boldrin, A., Malačič, V., Celio, M., Comici, C., Raicich, F., 2013. Exceptional dense water formation on the Adriatic shelf in the winter of 2012. Ocean Sci. 9, 561–572.
Millot, C., 1990. The Gulf of Lions' hydrodynamics. Cont. Shelf Res. 10, 885–894.
Mortlock, R.A., Froelich, P.N., 1989. A simple method for the rapid determination of biogenic opal in pelagic sediments. Deep-Sea Res. 36, 1415–1426.
Ogston, A.S., Drexler, T.M., Puig, P., 2008. Sediment delivery, resuspension, and transport in two contrasting canyon environments in the southwest Gulf of Lions. Cont. Shelf Res. 28, 2000–2013.
Pak, H., 1983. Fluctuations of beam-attenuation coefficient in the lowest 2 m on the continental rise off Nova Scotia. Mar. Geol. 51, 77–97.
Pak, H., Zaneveld, J.R.V., 1983. Temporal variations of beam attenuation coefficient on the continental rise off Nova Scotia. J. Geophys. Res. 88, 4427–4432.
Palanques, A., Durrieu de Madron, X., Puig, P., Fabres, J., Guillén, J., Calafat, A., Canals, M., Heussner, S., Bonnin, J., 2006. Suspended sediment fluxes and transport processes in the Gulf of Lions submarine canyons. The role of storms and dense water cascading. Mar. Geol. 234, 43–61.
Palanques, A., Guillén, J., Puig, P., Durrieu de Madron, X., 2008. Storm-driven shelf-to-canyon suspended sediment transport at the southwestern end of the Gulf of Lions. Cont. Shelf Res. 28, 1947–1956.
Palanques, A., Puig, P., Latasa, M., Scharek, R., 2009. Deep sediment transport induced by storms and dense shelf-water cascading in the Northwestern Mediterranean basin. Deep-Sea Res. I 56, 425–434.
Palanques, A., Puig, P., Guillén, J., Durrieu de Madron, X., Latasa, M., Scharek, R., Martin, J., 2011. Effects of storm events on the shelf-to-basin sediment transport in the southwestern end of the Gulf of Lions (Northwestern Mediterranean). Nat. Hazards Earth Syst. Sci. 11, 1–8.
Palanques, A., Puig, P., Durrieu de Madron, X., Sánchez-Vidal, A., Pasqual, C., Martín, J., Calafat, A., Heussner, S., Canals, M., 2012. Sediment transport to the deep canyons and open-slope of the western Gulf of Lions during the 2006 intense cascading and open-sea convection period. Prog. Oceanogr. 106, 1–15.
Pasqual, C., Sanchez-Vidal, A., Zúñiga, D., Calafat, A., Canals, M., Durrieu de Madron, X., Puig, P., Heussner, S., Palanques, A., Delsaut, N., 2010. Flux and composition of settling particles across the continental margin of the Gulf of Lion: the role of dense shelf water cascading. Biogeosciences 7, 217–231.
Perdue, E.M., Koprivnjak, J.F., 2007. Using the C/N ratio to estimate terrigenous inputs of organic matter to aquatic environments. Estuar. Coast. Shelf Sci. 73, 65–72.
Puig, P., Palanques, A., Orange, D.L., Lastras, G., Canals, M., 2008. Dense shelf water cascades and sedimentary furrow formation in the Cap de Creus Canyon, northwestern Mediterranean Sea. Cont. Shelf Res. 28, 2017–2030.
Puig, P., Palanques, A., Martín, J., Ribó, M., Font, J., 2012. Eventos de resuspensión de sedimento en el ascenso continental del margen Mediterráneo noroccidental. GeoTemas 13, 1840–1843.
Puig, P., Durrieu de Madron, X., Salat, J., Schroeder, K., Martín, J., Karageorgis, A.P., Palanques, A., Roullier, F., Lopez-Jurado, J.L., Emelianov, M., Moutin, T., Houpert, L., 2013. Thick bottom nepheloid layers in the western Mediterranean generated by deep dense shelf water cascading. Prog. Oceanogr. 111, 1–23.
Ribó, M., Puig, P., Palanques, A., Lo Iacono, C., 2011. Dense shelf water cascades in the Cap de Creus and Palamós submarine canyons during winters 2007 and 2008. Mar. Geol. 284 (1–4), 175–188.
Richardson, M.J., Weatherly, G.L., Gardner, W.D., 1993. Benthic storms in the Argentine Basin. Deep-Sea Res. 40, 975–987.
Rubino, A., Romanenkov, D., Zanchettin, D., Cardin, V., Hainbucher, D., Bensi, M., Boldrin, A., Langone, L., Miserocchi, S., Turchetto, M., 2012. On the descent of dense water on a complex canyon system in the southern Adriatic basin. Cont. Shelf Res. 44, 20–29.
Salat, J., Puig, P., Latasa, M., 2010. Violent storms within the Sea: dense water formation episodes in the NW Mediterranean. Adv. Geosci. 26, 53–59.
Salomon, W., Mook, W.G., 1981. Field observation of the isotope composition of particulate organic carbon in the southern North Sea and adjacent estuaries. Mar. Geol. 4, M11–M20.
Sanchez-Vidal, A., Pasqual, C., Kerherve, P., Heussner, S., Calafat, A., Palanques, A., Durrieu de Madron, X., Canals, M., Puig, P., 2009. Across margin export of organic matter by cascading events traced by stable isotopes, northwestern Mediterranean Sea. Limnol. Oceanogr. 54, 1488–1500.
Schott, F., Leaman, K.D., 1991. Observations with Moored Acoustic Doppler Current Profilers in the Convection Regime in the Golfe du Lion. J. Phys. Oceanogr. 21, 558–574.
Schroeder, K., Millot, C., Bengara, L., Ben Ismail, S., Bensi, M., Borghini, M., Budillon, G., Cardin, V., Coppola, L., Curtil, C., Drago, A., El Moumni, B., Font, J., Fuda, J.L., García-Lafuente, J., Gasparini, G.P., Kontoyiannis, H., Lefevre, D., Puig, P., Raimbault, P., Rougier, G., Salat, J., Sammari, C., Sánchez Garrido, J.C., Sanchez-Roman, A., Sparnocchia, S., Tamburini, C., Taupier-Letage, I., Theocharis, A., Vargas-Yáñez, M., Vetrano, A., 2013. Long-term monitoring programme of the hydrological variability in the Mediterranean Sea: a first overview of the HYDROCHANGES network. Ocean Sci. 301–324.
Severin, T., Conan, P., Durrieu de Madron, X., Houpert, L., Oliver, M.J., Oriol, L., Caparros, J., Ghiglione, J., Pujo-Pay, M., 2014. Impact of open-ocean convection on nutrients, phytoplancton biomass and activity. Deep-Sea Res. 94, 62–71.
Stabholz, M., Durrieu de Madron, X., Khripounoff, A., Canals, M., Taupier-Letage, I., Testor, P., Heussner, S., Kerhervé, P., Houpert, L., Delsaut, N., 2013. Impact of open-sea convection on particulate fluxes and sediment dynamics in the deep basin of the

Gulf of Lions. Biogeosciences 10, 1097–1116.
Stommel, H., 1972. Deep winter-time convection in the western Mediterranean Sea. In: Gordon, A.L. (Ed.), Studies in Physical Oceanography. Vol 2. Gordon and Breach, pp. 207–218.
Tamburini, C., Canals, M., Durrieu de Madron, X., Houpert, L., Lefèvre, D., et al., 2013. Deep-sea bioluminescence blooms after dense water formation at the ocean surface. PLoS One 8 (7), e67523.
Tesi, T., Puig, P., Palanques, A., Goñi, M.A., 2010. Lateral advection of organic matter in cascading-dominated submarine canyons. Prog. Oceanogr. 84, 185–203.
Testor, P., Gascard, J.C., 2003. Large scale spreading of deep and intermediate water in the western Mediterranean Sea by submesoscale and mesoscale coherent eddies. J. Phys. Oceanogr. 33, 75–87.
Testor, P., Gascard, J.C., 2006. Post-convection spreading phase in the Northwestern Mediterranean Sea. Deep-Sea Res. I Oceanogr. Res. Pap. 53, 869–893.
Trincardi, F., Foglini, F., Verdicchio, G., Asioli, A., Correggiari, A., Minisini, D., Piva, A., Remia, A., Ridente, D., Taviani, M., 2007. The impact of cascading currents on the Bari Canyon System, SW-Adriatic margin (Central Mediterranean). Mar. Geol. 246, 208–230.
Turchetto, M., Boldrin, A., Langone, L., Miserocchi, S., Tesi, T., Foglini, F., 2007. Particle transport in the Bari Canyon (southern Adriatic Sea). Mar. Geol. 246, 231–247.
Wright, C.J., Scott, R.B., Furnival, D., Ailliot, P., Vermet, F., 2013. Global observations of ocean-bottom subinertial current dissipation. J. Phys. Oceanogr. 43, 402–417.